Identification of genetic determinants involved in multicellular aggregates formation in *Burkholderia multivorans*

Catarina Reis, IBB - Institute for Bioengineering and Bioscience, Instituto Superior Técnico

Abstract: Microorganisms can live freely or as multicellular aggregates. These aggregates are of great importance, especially in clinical settings, due to the increased ability to prevail in diverse environmental conditions. *Burkholderia cepacia* complex are some of the bacteria capable of forming multicellular aggregates, contributing to the establishment of chronic infection in cystic fibrosis (CF) patients, often leading to decreased lung function. However, the molecular mechanisms involved in the formation of cellular aggregates by these bacteria are mostly unknown. Here, we have characterized two *Burkholderia multivorans* sequential isolates from a CF patient, in which P0426-1 was able to form aggregates and P0426-2, not. Comparison of their genome sequence identified 4 SNP mutations in coding sequences, 2 indels, and a large deletion in P0426-2. One of the SNPs was in a gene encoding the putative lactonase YtnP. These enzymes are known to regulate quorum sensing communication by degrading N-acyl-homoserine lactones (AHLs). Expression of YtnP-85R from isolate P0426-2 into isolate P0426-1 resulted in the reduction of aggregates biomass and affected aggregates structure. Similarly, expression of YtnP-85R in two different *B. multivorans* strains, P0213-1 and P0148-1, which form aggregates, caused alterations in aggregates structure in P0213-1, but not in P0148-1. To determine the range of AHLs degraded by this putative lactonase, the recombinant His_6YtnP-85S was successfully overexpressed and purified in *E. coli*, but no enzyme activities were done. Further work needs to be performed in order to characterize this novel lactonase enzyme, namely its possible role in regulating gene expression and pathogenesis in *Burkholderia*.

Keywords: *Burkholderia multivorans,* Planktonic cellular aggregates, Lactonase, Cystic fibrosis.

Introduction

One of the most common hereditary diseases affecting populations with European descent is cystic fibrosis (CF), a recessive disease caused by mutations in the cystic fibrosis transmembrane conductance regulator (CFTR) gene [1,2]. CFTR protein is a part of the ATP-binding cassette (ABC) family of membrane proteins responsible for the transport of chloride ions through the cell membrane, helping maintain an equilibrium in exocrine organ systems like the pancreas, lungs, liver, etc, being lung disease the major cause of morbidity and mortality in CF patients [3-5]. What happens in the lungs of CF patients is that mucus clearance is affected due to the depletion of the airway surface liquid, which will increase the prevalence of bacterial infections that can lead to respiratory failure [6,7].

Microorganisms have the ability to form sessile communities in many types of surfaces. Biofilms can be found in a wide range of surfaces and conditions, being composed of microbial communities, water, and polysaccharides, among other macromolecules, providing bacteria with protection against external factors, such as antibiotics [8]. There are two types of multicellular aggregates, surface-attached biofilms and planktonic cellular aggregates, which happens when bacteria adhere to each other instead of a surface [9]. Biofilms are frequently related with a lot of diseases caused by pathogens. *Burkholderia cepacia* complex (Bcc) are bacteria with the ability to form multicellular aggregates, allowing them to cause persistent infections that can often lead to severe damage on the lungs of CF patients [10].

Seeing that many cystic fibrosis isolates of *B. multivorans* have the ability to form multicellular aggregates, so to study the molecular mechanisms involved in the formation of this aggregates, two sequential *B. multivorans* isolates from the same CF patient were studied. The first isolate had the ability to form aggregates and the second was lacking this ability, being only 7 mutations between them, which study could help to better understand multicellular aggregate formation in Bcc and the mechanisms that may be involved in it.

Materials and methods

Bacterial strains and growth conditions

Bacterial strains and plasmids used in this study are listed in Table S1. *Escherichia coli* was grown at 37ºC in Lennox Broth (LB) with or without agar, supplemented with kanamycin (50 µg/ml) or chloramphenicol (25 µg/ml) when required to maintain selective pressure. *Burkholderia multivorans* strains were grown in LB, SCFM

(synthetic cystic fibrosis medium) (Palmer *et al.* 2007) or SM medium (12.5 g/liter $Na_2HPO_4.2H_2O$, 3 g/liter KH_2PO_4, 1 g/liter K_2SO_4, 1 g/liter NaCl, 0.2 g/liter $MgSO_4.7H_2O$, 0.01 g/liter $CaCl_2.2H_2O$, 0.001 g/liter $FeSO_4.7H_2O$, 1 g/liter yeast extract, 1 g/liter casamino acids, pH 7.2), supplemented with 20 g/liter of D-mannitol, and the following antibiotics: chloramphenicol (250 µg/ml) and Gentamicin (40 µg/ml) when required to maintain selective pressure, at 37ºC with 180 rpm of orbital agitation.

DNA manipulation and cell transformation techniques

Genomic DNA extraction from *B. multivorans* strains was performed using a protocol previously described [11]. Plasmid DNA isolation and purification, DNA restriction, agarose gel electrophoresis, DNA amplification by PCR, and *E. coli* transformation were performed using standard procedures (primers are described in Table S2) [12]. *E. coli* electrocompetent cells were transformed by electroporation using a Bio-Rad Gene Pulser II system (400 Ω, 25 µF, 2.5 kV) and grown for 1 hour before being plated on selective medium.

For triparental conjugation,

the donor strain was inoculated in 3 mL of LB with chloramphenicol, the helper strain was inoculated in 3 mL of LB with kanamycin and the recipient strain was inoculated in 3 mL of LB without antibiotic. The cultures were incubated, during 5 hours, at 37ºC with 250 rpm of orbital agitation. After incubation, 1 mL of recipient was mixed with 1 mL of each helper and donor. The final mixture was transferred to a LB plate and incubated for 24 hours at 30ºC. This conjugation mixture was, then, plated onto LB plates supplemented with 250 µg/ml chloramphenicol and 40 µg/ml gentamicin, and incubated at 37ºC for 24 hours.

Real-Time qPCR

Isolates under study were inoculated in SM medium with an initial OD640nm 0.1, and incubated at 37ºC with 180 rpm of orbital agitation. Samples were collected at 4, 8 and 24 hours and RNA was extracted with RNeasy Mini Kit by Qiagen, following an optimized procedure, based on manufacturer recommendations. To avoid contamination of genomic DNA, a step of DNA digestion was performed using Thermo Scientific DNase I, RNase-free, an endonuclease that digests single- and double-stranded DNA. RNA samples were stored immediately after extraction at -80ºC. Real-Time qPCR was performed using a relative quantification method based on a one-step protocol. A dilution of the RNA samples was performed in order to obtain 12.5 ng of RNA in 50 µl, as well as 1:10 dilutions of the primers. For each well of the 96-well plate, 5.6 µl of DEPC-treated H2O, 1.6 µl of the primer solution and 2 µl of RNA, 10 µl of One-step NZY qPCR Green master mix (2x) and 0.8 µl of ROX and NZYRT mix from NZYTech® were added.

Growth curves

Cells from an overnight culture were inoculated in 50 mL of fresh SM medium (OD640nm 0.1). The culture was incubated at 37ºC with 180 rpm of orbital agitation. OD640nm readings were taken over time during 7 hours and then at 24 and 48 hours. Each growth curve was performed in duplicate.

Quantification of cellular aggregates and free cells

Each bacterial mutant was grown overnight in 3 mL of SM medium at 37ºC with 250 rpm of orbital agitation. Suspensions with OD640nm 0.1, were prepared in Erlenmeyers containing fresh SM medium and incubated at 37ºC with 180 rpm of orbital agitation during 48 hours. The free cells and planktonic aggregates present in the Erlenmeyer were separated in 50 mL flacon tubes, and later placed on pre-weighted 2 mL Eppendorf tubes by preforming multiple centrifugations. These eppendorf tubes were then left to dry at 60°C for 72 hours. After the tubes were dried they were weighted again.

Microscopy analysis

B. multivorans strains grown in SM medium for 48 hours were visualized on Zeiss Axioplan microscope, equipped with a Axiocam 503 color Zeiss camera, using a 10x 0.3 NA objective, and controlled with the Zen software.

Overexpression and purification of YtnP protein

The *ytnP* gene from isolate P0426-1 was cloned using the plasmid pET23a+ resulting in the plasmid pCR21-4. This plasmid was transformed into *E. coli* BL21 (DE3) and the His_6-tagged protein was overexpressed by growing transformed *E. coli* BL21 (DE3) in 50 mL of LB liquid medium supplemented with 100 µg/mL ampicillin at 37°C and with orbital agitation (250 rpm). Protein overexpression was induced by the addition of 0.4 mM of IPTG to the growth medium and cultures were incubated for 4 hours, under the same conditions. Bacteria were then harvested by centrifugation for 5 min at 7000×g and 4°C. The resulting pellet was resuspended in 6 mL sonication buffer (Phosphate Buffer 1x (pH 7.4), 10 mM Imidazole). The overexpression evaluated by SDS-PAGE analysis. Cell suspensions were lysed by ultrasonic vibration with a Branson sonifier 250 (Branson), using 6 sonication cycles of 30 s each at 40 % duty cycle. After sonication, cell debris were removed by centrifugation at 12.000×g for 30 min at 4°C and the supernatant was collected to a new tube. The His6-tagged protein was purified through affinity chromatography using HisTrap FF columns (Amersham Biosciences). The HisTrap FF column was washed with 5 ml distilled water and then regenerated with 10 ml of Solution C. After being regenerated, the column was charged with 0.5 ml of 0.1 M nickel sulphate salt solution and then washed again with 5 ml of distilled water. To purify the protein the column was balanced with 10 ml Buffer I and then

the sample was fully applied. A constant increasing gradient of imidazole concentration was used to elute the protein, with imidazole concentrations varying form 10 mM to 500 mM. One by one, 5 ml of each buffer were applied to the column and 1ml aliquots were recovered during the elution. To later determine the fractions containing the protein of interest, 20 µl of each collected aliquot were analysed by SDS-PAGE.

Comparative sequence analysis

The comparative sequence analysis was performed using MEGA-X v.10.5.0. The protein sequences of each gene cluster were first concatenated and independently aligned by Clustal.

Statistical analysis

The statistical significance of differences in the data was determined using the one-way analysis of variance (ANOVA) followed by Dunnett's multiple comparisons test which were performed using GraphPad Prism software 8.0.1 for Windows (GraphPad Software, San Diego California USA, www.graphpad.com). Differences were considered statistically significant for P-values lower than 0.05.

Results and Discussion

In vitro *quantification of aggregate formation by* Burkholderia multivorans *P0426-1 and P0426-2.*

A longitudinal series of 21 isolates recovered from the cystic fibrosis patient P0426 between 1997 and 2004 and available from the Canadian *Burkholderia cepacia complex* research and referral repository (CBCCRRR) was available for this study. Out of these isolates, the first one has the ability to form large multicellular aggregates while the remaining ones were incapable of forming these aggregates or formed very small ones [13]. The first isolate P0426-1 and the second, P0426-2, are sequential isolates recovered a month apart of each other, being the first able to form large aggregates whilst the second could not form any. To quantify the planktonic cellular aggregates formed by P0426-1 and P0426-2, both isolates were grown in SM medium, which has high carbon to nitrogen ratio and in SCFM medium that mimetizes nutrients available in the CF lung environment

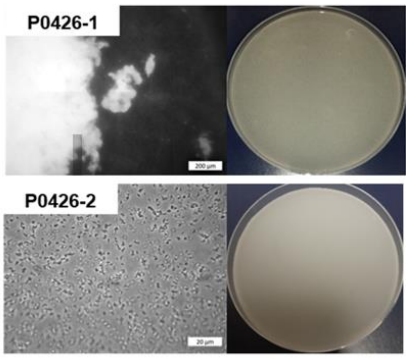

A

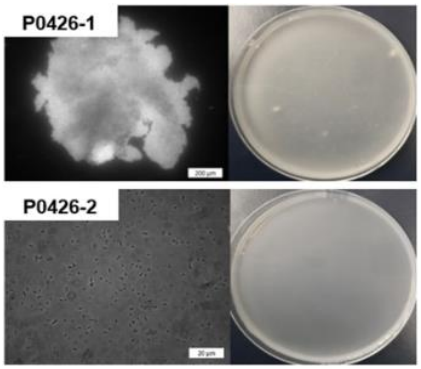

B

Figure 1: Screening for aggregate formation by *B. multivorans* clinical isolate P0426-1 and P0426-2 in both SM (A) and SCFM medium (B).

B. multivorans P0426-1 grows both as free cells and cellular aggregates (Fig.1), while *B. multivorans* P0426-2 was not able to form planktonic aggregates.

Although using SCFM might provide a better depiction of the formation of multicellular aggregates by isolate P0426-1 in CF sputum, the results were very similar to SM medium (Fig. 1B).

To obtain a better perception of the differences in aggregate formation ability by both strains, the planktonic cellular aggregates were quantified by weighting the dry biomass of both planktonic cells and aggregates separately.

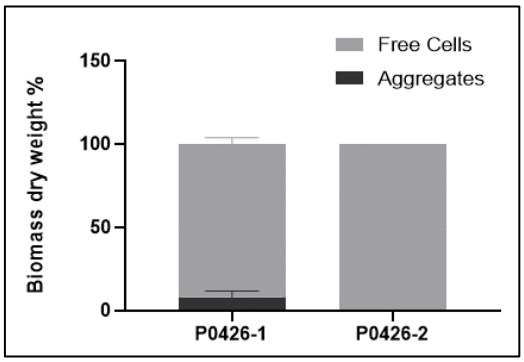

Figure 2: Quantification of cellular aggregates and free cells of P0426-1 and P0426-2 grown in SM medium at 37˚C, 180 rpm for 48h.. Error bars correspond to the standard deviations of the mean values of three independent experiments.

As can be seen in Figure 2 isolate P0426-1 produces around 8% of the biomass as planktonic aggregates, being the majority of the biomass produced as free cells. From the isolate P0426-2 we were unable to obtain aggregates, having 100% of the biomass in the form of free cells.

This results confirm previous observations on the ability of the first isolate P0426-1 to form multicellular aggregates while isolate P0426-2 seem to form only free cells.

Genomic alterations between B. multivorans *isolates P0426-1 and P0426-2*

To understand this inability to form planktonic aggregates by *B. multivorans* P0426-2 and since the sequence of the genome of both isolates was available, the differences between them were analyzed (Table S3). In comparison to isolate P0426-1, isolate P0426-2 has four SNP mutations in the coding region of: a gene encoding a putative quorum-quenching lactonase (YtnP), a purine efflux pump (PbuE), a multidrug resistance protein (Stp), and an outer membrane protein (TtgC). This caused nonsynonymous mutations and except for protein Stp they are present in all isolates of the longitudinal series. Other differences between the two isolates are two small indel mutations in intergenic regions, being the genes that could be affected by the 7 base-pairs insertion the bceT gene encoding the UTP-glucose-1-phosphate uridylyltransferase (BceT) and/or the acyltransferase (BceU), both involved in cepacian biosynthesis. The 10 nucleotides deletion might affect a LysR-type transcriptional regulator (GltR) and/or an alanyl-tRNA synthetase (AlaS). A large deletion of approximately 44 kb is also present in P0426-2 as well as 6 other isolates and includes mainly genes encoding hypothetical proteins.

Lactonases are known quorum quenching enzymes that can affect biofilm formation by degrading AHLs, which disrupts quorum sensing [14]. TtgC is an outer membrane channel part of the TtgABC efflux system. The role of efflux pumps in biofilm formation has been described previously for other bacteria, including *E.coli*, *Klebsiella pneumoniae*, and *Salmonella enterica* [15,16]. PbuE is a purine efflux pump involved in the efflux of purine ribonucleosides. This protein has been proven to modulate the expression of two regulons, purR and G-box. As this HTH-type transcriptional repressor (PurR) is proven to be involved in biofilm formation in Staphylococcus aureus, a mutation on the PbuE protein could possibly have an effect in multicellular aggregate formation [17,18]. The Stp protein is a sugar transport protein that various studies have been successful in proving the involvement in the communication of certain bacteria with the host cells, mainly in stages such as adhesion, invasion and possibly biofilm formation [19]. The two indel mutation in intergenic region could be affecting the expression of the genes nearby. Since UTP-glucose-1-phosphate uridylyltransferase (BceT) enzyme is involved in the synthesis of the activated sugar-nucleotide UDP-D-Glucose, which is then the precursor for UDP-D-glucuronic acid and UDP-D-galactose, changes in the levels of these sugar nucleotides could affect the amount of cepacian being produced. The acetyltransferase BceU is involved in the decoration of the cepacian repeat-unit and could contribute to differences at the acetylation level of the final polymer [20]. Both changes could have an effect on biofilm formation as documented in several publications [21,22]. Some LysR-type transcriptional regulators have been implicated in quorum sensing regulation and to have an effect in biofilm formation [23]. Therefore, *gltR* might be important for biofilm formation. No involvement of alanyl-tRNA synthetase in biofilm formation has yet been reported.

The large deletion that occurred in isolate P0426-2 eliminates 62 genes encoding hypothetical proteins, but since some isolates having this region are also unable to produce aggregates, this mutation will not be considered in further studies.

From the mutation analysis, genes mutated in all isolates are our primary targets for being implicated in aggregate formation. In particular, we will investigate genes *ytnP* and *ttgC*, as described in the next sections.

Genetic complementation with ytnP *gene*

As the YtnP protein of isolate P0426-2 has an arginine residue at position 85 and is conserved in all its homologues, we hypothesized this would be the wild-type protein. Then, YtnP of isolate P0426-1 would perhaps be affected in its lactonase activity. In the absence or reduction of this activity the intracellular levels of AHLs in P0426-1 would be higher, leading perhaps to aggregate formation of a larger size due to the expression of genes implicated in this trait. Contrastly, in isolate P0426-2, the levels intracellular of AHLs would be lower and no multicellular aggregates would be formed. To test our hypothesis, the 1.3-Kb *ytnP* gene of isolate P0426-1 and P0426-2 was cloned into the pBBR1MCS broad-host-range vector, leading to the formation of pCR20-1 and pCR20-5 expressing the ytnP gene of P0426-1 and P0426-2, respectively. A complementation assay was performed in which the plasmid pCR20-5 and the empty vector were introduced into isolate P0426-1 and pCR20-1 and the empty vector into P0426- 2. Cells were grown in SM medium at 37ºC with 180 rpm of orbital agitation for 48 hours followed by inspection of aggregates formation.

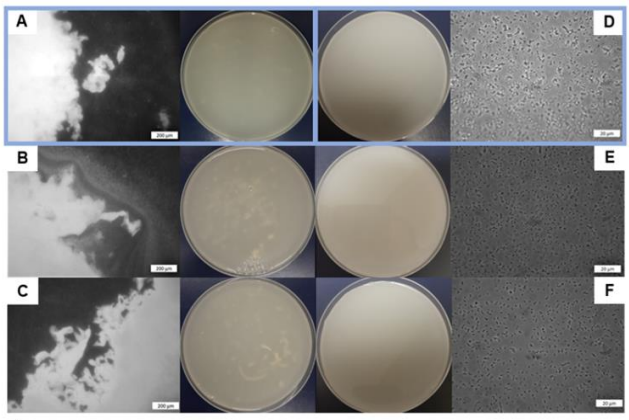

Figure 3: Screening for aggregate formation by P0426-1, P0426-2 expressing a different lactonase. A- P0426-1; **B-** P0426-1/pBBR1MCS; **C-** P0426-1/pCR20-5 (YtnP-85R); **D-** P0426-2; **E-** P0426-2/pBBR1MCS; **F-** P0426-2/pCR20-1 (YtnP-85S).

The microscopic and macroscopic appearance of the planktonic cellular aggregates can be seen in Figure 3. When compared with the parental isolate P0426-1, the introduction of the empty pBBR1MCS vector stimulated aggregates formation of larger size (compare Fig. 3A vs Fig. 3B). The expression of YtnP-85R in P0426-1 did not prevent aggregate formation, but the structure of the aggregates seems to be more compact and with more ramifications (compare Fig.3B vs Fig. 3C). Regarding isolate P0426-2, the introduction of the empty vector or expressing Ytnp-85S, as expected, did not have any impact since cells remained as free-cells (Fig. 3D-F).

To determine whether there were differences in aggregate formation by the complementation of the isolates, the percentage of biomass dry weight recovered from both aggregates and free cells is shown in Figure 4.

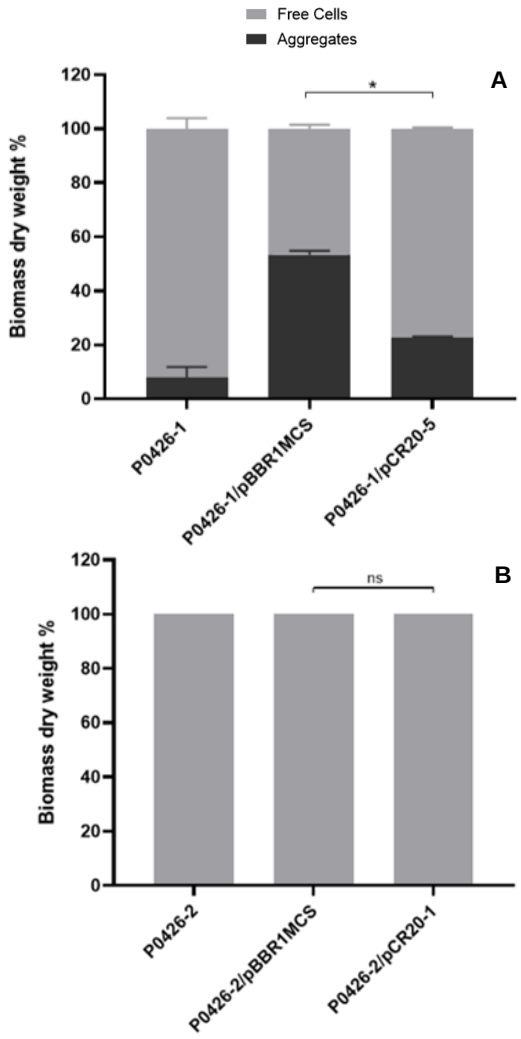

Figure 4: Quantification of cellular aggregates and free cells. A- P0426-1 parental and complemented; **B-** P0426-2 parental and complemented. Error bars correspond to the standard deviation. Significance level (one-way ANOVA followed by Dunnett's multiple comparison test) between cellular aggregates and free cells of the parental (P0426-1 and P0426-2) and cellular aggregates and free cells of the complemented isolates was determined: *, P <0.05; ns, not statistically significant.

Confirming the macroscopic observation, the parental isolate P0426-1 produces 8% of its biomass in the form of cellular aggregates, while with the empty vector this value is considerably higher (53%). The comparison of the aggregates biomass between P0426-1/pBBR1MSC and P0426-1-YtnP-85R showed a statistically significant reduction (53% to 22%) for the isolate expressing YtnP-85R (Fig. 4A). As expected, no aggregates were obtained from isolate P0426-2 with or without the expression of YtnP-85S (Fig. 4B). This result suggests that YtnP-85R expression in P0426-1 might have affected both the structure of the aggregates and their relative amount.

To determine whether the lactonase enzymes under study would have impact in aggregates formation in other *Burkholderia*, we have chosen isolate P0213-1 and P0148-1 recovered from two different CF patients. Isolates P0213-1 and P148-1, which lack this gene in their genome, were grown in SM medium at 37ºC with 180 rpm of orbital agitation for 48 hours. Aggregates were visualized macroscopically in the broth and at the microscope (Fig. 5A and E, respectively). Then, the empty vector, as well as the plasmids expressing YtnP-85S or YtnP-85R were mobilized to each of the isolates.

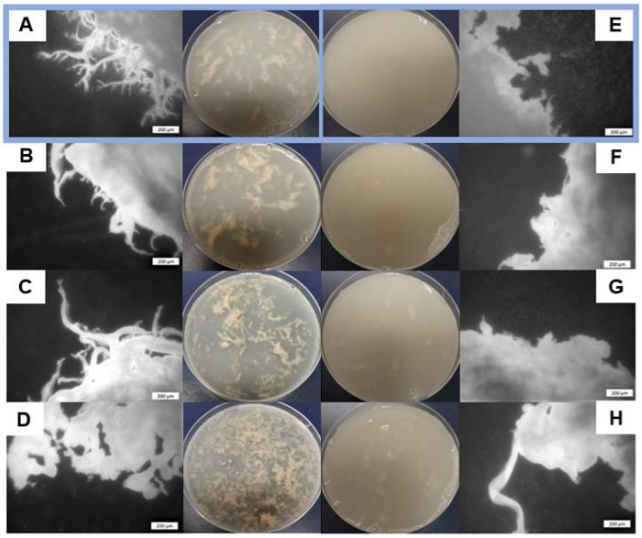

Figure 5: Screening for aggregate formation by P0213-1, P0148-1 and respective complemented mutants. A- P0213-1; **B-** P0213-1/pBBR1MCS; **C-** P0213-1/pCR20-1 (YtnP-85S); **D-** P0213-1/pCR20-5 (YtnP-85R); **E-** P0148-1; **F-** P0148-1/pBBR1MCS **G-** P0148-1/pCR20-1 (YtnP-85S); **H-** P0148-1/pCR20-5 (YtnP-85R).

As shown in Figure 5, all strains were able to form planktonic cellular aggregates. When comparing the parental strain P0213-1, with the respective complemented form, some phenotypic/morphologic changes can be seen. The P0213-1 isolate expressing YtnP-85R (Fig. 5D) presented the strongest phenotypic difference in comparison with the other 2 strains. Instead of the large aggregates seen in the other strain (Fig. 5A-C), P0213-1 expressing YtnP-85R produced higher number of small aggregates. The microscopic shape of the

planktonic cellular aggregates formed by the expression of the YtnP-85R lactonase was significantly different from the other strains, appearing to have lost the ability to form the ramifications that can be seen in the other P0213-1 strains. A similar analysis of isolate P0148-1 expressing both lactonase variants did not show significant difference in the structure of the aggregates (Fig. 5E-H).

The planktonic cellular aggregates and free cells were quantified by weighing the dry biomass, in order to better visualise the differences between the isolates.

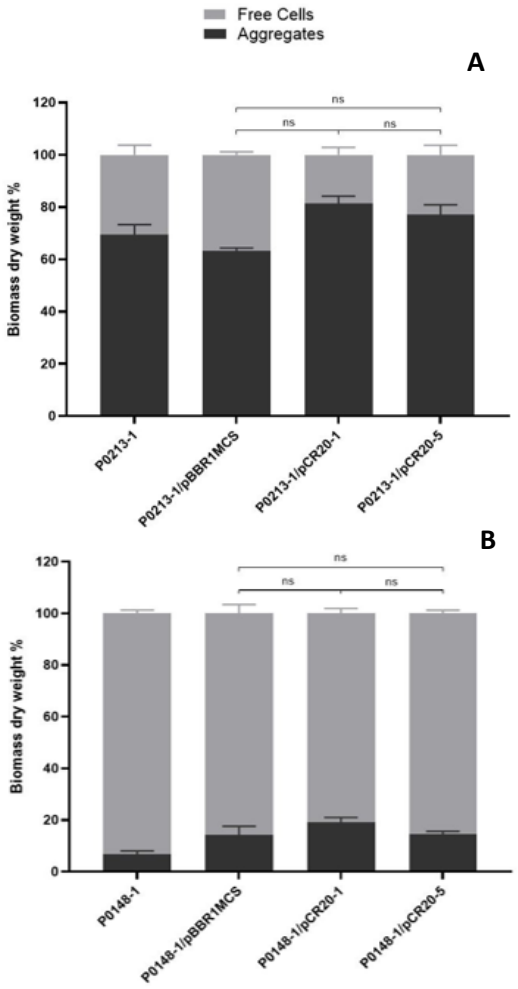

Figure 6: Quantification of cellular aggregates and free cells. A- P0213-1 parental and complemented; **B-** P0148-1 parental and complemented. Error bars correspond to the standard deviation. Significance level (one-way ANOVA followed by Dunnett's multiple comparison test) between cellular aggregates and free cells of the parental (P0213-1 and P0148-1) and cellular aggregates and free cells of the complemented isolates was determined: ns, not statistically significant.

Analysis of Figure 6A allows to visualize an increase of aggregates biomass in the P0213-1 strain expressing both lactonase variants, although this increase was not statistically significant when compared to the presence of the empty vector. Expression of the two lactonase variants in isolate P0148-1 also did not have significant impact in aggregate formation when compared to the strain with the empty vector (Fig. 6B).

Altogether, our data suggests that expression of YtnP-85R affected aggregate morphology in P0213-1, but no difference was observed in strain P0148-1.

Lactonases, as previously mentioned, have been proven to be able to disrupt QS in several bacterial species. However, lactonase efficiency in inhibiting QS depends on several factors, such as AHL hydrolytic activity levels and the specificity of the lactonase being studied. Some lactonases are able to completely inhibit biofilm formation while other only slightly decrease the formation and/or the size of the aggregates [24]. This could explain the phenotype that can be seen in P0213-1 expressing YtnP-85R (Fig. 5D). Although there was not a decrease in multicellular aggregate formation, the size of the aggregates decreased significantly which could be suggest YtnP-85R is active but the specificity to this AHLs is low.

Lactonases can have different specificity and different biological roles. Some lactonases act intracellularly playing a role in self-regulation of AHL-mediated quorum sensing. It has already been shown that the fine-tunning of AHL concentration in *P. aeruginosa* is achieved by AHL acylase activity [25]. Contrastly, extracellular lactonases respond to QS signals produced by competitors living within the same niche giving the quorum quenching producer a competition advantage. Such an example of this type of lactonase was recently characterized in *Burkholderia cepacia* BCC4135 [26]. This strain produces the lactonases YtnP and Y2-aiiA, being the first intracellular and the second extracellular. Analysis of the enzymatic potential showed that YtnP has a higher preference for short and middle-long chain AHLs, while the Y2-aiiA was efficient against both short- and long-chained AHLs. Therefore, the authors proposed that the intracellular YtnP might be involved in self-regulation of AHL-mediated QS while Y2-aiiA, by displaying broader substrate specificity may have the ability to respond to different QS signals produced by competitors. The YtnP homolog of *B. multivorans* characterized in this study shows low homology to Y2-aiiA (29% similarity) and YtnP (30% similarity) from *B. cepacia* and is a new putative lactonase.

Overexpression and purification of YtnP-85S protein

With the aim of characterizing the biochemical activity of this lactonase enzyme, we envisaged the cloning of the two gene alleles, and protein expression and purification. Nevertheless, due to time limitations only one of the genes was clones. To this purpose, the 1.3-Kb PCR fragment from P0426-1 isolate was amplified and cloned into the expression vector pET-23a(+) under the control of the T7 promoter, creating pCR21-4 (Table S1). The overexpression of the protein as a His-tagged derivative was accomplished by

introduction of the plasmid pCR21-4 into *E. coli* BL21 (DE3) cells. The transformed *E. coli* DL21 (DE3) were grown in LB medium and various conditions were tested to improve the amount of protein expressed and the ones that showed higher levels of the His-tagged protein were selected. Although a high overexpression of YtnP protein was not achievable, the best condition for the protein expression in *E. coli* BL21 (DE3) was at 37º C with 100 µg/L of ampicillin, with an IPTG induction time of 4 hours.

The overexpressed His_6-tagged protein was analysed by SDS-PAGE (Figure 7A). Although a clear band corresponding to the predicted protein size (31 kDa) was not visible in lanes 4 and 5, its location is indicated with and arrow.

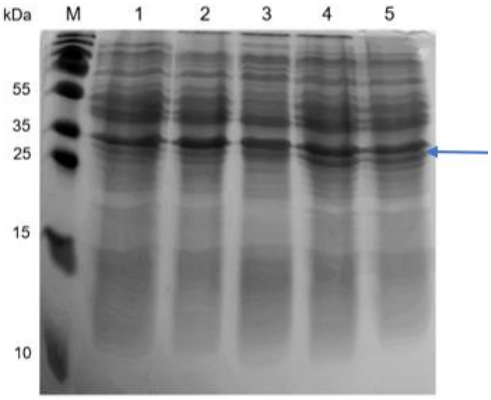

Figure 7: 15% SDS-PAGE gel with YtnP overexpression assay samples. Lane M - PageRuler™ Plus prestained protein ladder (Thermo Scientific); Lane 1 – *E. coli* BL21 (DE3); Lane 2 - pET-23a(+); Lane 3 – pCR21-4 with 0mM IPTG (t0); Lane 4 – pCR21-4 0.4 mM IPTG (t4); Lane 5 – pCR21-4 0.4 mM IPTG (t24).

The purification of the recombinant protein was performed using nickel affinity chromatography. The extract sample was fully applied to the column and a constant increasing gradient varying form 10 mM to 500 mM of imidazole concentration was used to elute the protein. The eluted fraction from the column were analysed through SDS-PAGE (Figure 8), with the protein present in 7 of the fractions. The fraction containing higher concentration of the YtnP protein was the third fraction eluted with the buffer containing 100 mM of imidazole. Small amounts of contaminants were present in most of the fractions recovered with the protein, being the fifth fraction eluted with the buffer containing 100 mM of imidazole the only one were no contaminants were present.

The purified YtnP protein could be used in further studies to better understand the function of this lactonase and the importance of these types of enzymes in inhibiting virulence in some bacterial species by interfering with their QS systems. But, before that, there is still room for improvement of its expression and further purification. For example, gel filtration chromatography, should be assayed.

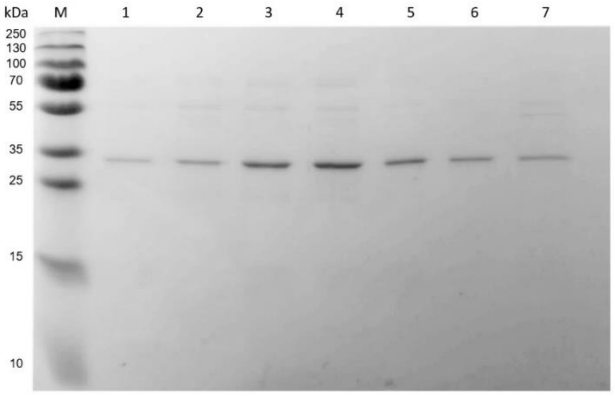

Figure 8: Analysis by SDS-PAGE of His-tagged YtnP protein purification by nickel affinity chromatography. Lane M - PageRuler™ Plus prestained protein ladder (Thermo Scientific); Lane 1 - 50(3) mM imidazole; Lane 2- 100(1) mM imidazole; Lane 3- 100(2) mM imidazole; Lane 4- 100(3) mM imidazole; Lane 5- 100(4) mM imidazole; Lane 6- 100(5) mM imidazole; Lane 7- 300(1) mM imidazole.

Genetic complementation with the ttgC *gene*

The 1.6-Kb *ttgC* gene and its own promotor from each clinical isolate was cloned into the pBBR1MCS broad-host-range vector, in order to study the possible role of this outer membrane protein in the formation of multicellular aggregates. A complementation assay was performed to test whether this change in amino acid from a threonine to an alanine might have caused the impairment of multicellular aggregate formation in P0426-2. The plasmid pCR21-3, together with the empty vector was introduced into P0426-1 and pCR21-2 into P0426- 2. Cells were grown in SM medium at 37ºC with 180 rpm of orbital agitation for 48 hours followed by inspection of aggregates formation.

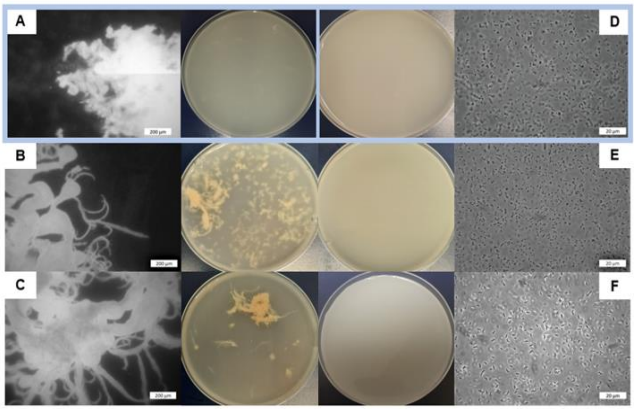

Figure 9: Screening for aggregate formation by P0426-1, P0426-2 expressing a different outer membrane protein TtgC. A- P0426-1; **B-** P0426-1/pBBR1MCS; **C-** P0426-1/pCR21-3 (TtgC-503A); **D-** P0426-2; **E-** P0426-2/pBBR1MCS; **F-** P0426-2/pCR21-2 (TtgC-503T).

The microscopic and macroscopic appearance of the planktonic cellular aggregates can be seen in Figure 9. In the complementation of P0426-1 none of the strains showed significant differences microscopically, but the number of aggregates seem

very different. The complementation of P0426-2 there were also no phenotypical changes when comparing the respective parental strain. For a better understanding of the differences in aggregate formation by the complementation of the isolates, the percentage of biomass dry weight recovered from both aggregates and free cells was determined.

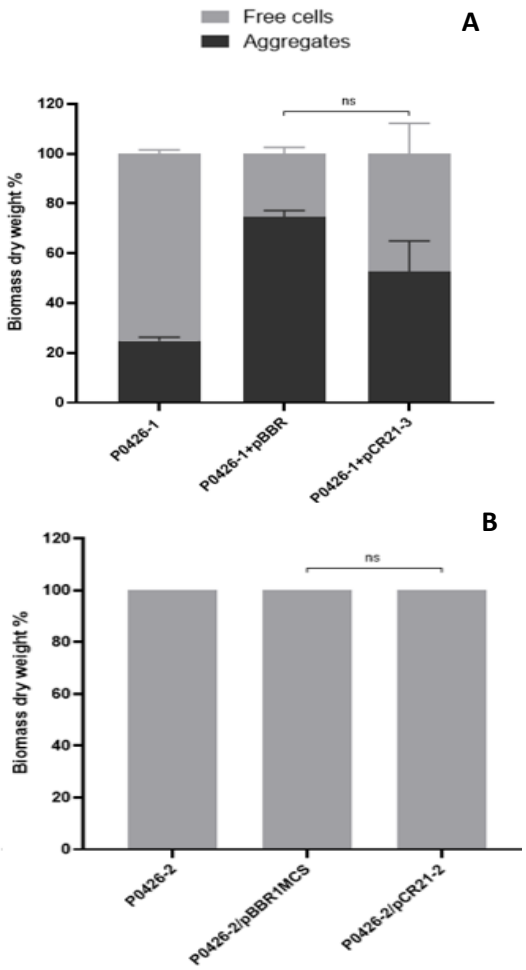

Figure 10: Quantification of cellular aggregates and free cells. A- P0426-1 parental and complemented; **B-** P0426-2 parental and complemented. Error bars correspond to the standard deviation. Significance level (one-way ANOVA followed by Dunnett's multiple comparison test) between cellular aggregates and free cells of the parental (P0426-1 and P0426-2) and cellular aggregates and free cells of the complemented isolates was determined: ns, not statistically significant.

As depicted in Figure 10A, the presence of the empty vector in isolate P0426-1 increased in the formation of planktonic cellular aggregates, when compared the parental strain, but the expression of TtgC-503A led to a decrease of aggregate formation. Complementation of P0426-2 with the ttgC gene from P0426-1 (TtgC-503T) also did not alter the proportion between free cells and aggregates (Fig. 10B), since none of the complemented were able to form aggregates.

In conclusion, expression of the TtgC-503A in P0426-1 seems to have reduced aggregate biomass, but the aggregates were generally of a larger size, suggesting a possible (but small) role of this protein in aggregate formation.

Gene expression analysis by real-time quantitative RT-PCR

A RT-qPCR assay based on SYBR Green detection was performed to assess the expression of the four genes that might be affected by the two mutation in intergenic, and possibly, promotor regions present between the two isolates. Each reaction was performed once for the three different times (4, 8 and 24 hours of growth), and three replicates were performed for each gene being analysed.

The method used to analyse the data was the comparative C_T method ($\Delta\Delta C_T$ Method). The C_T is described as the number of cycles that are necessary for the fluorescent signal of the SYBR Green to cross the threshold and is inversely proportional to the quantity of target mRNA present in the sample.

As previously mentioned, the RNA was extracted in 3 different point (4, 8 and 24 hours), a digestion with DNase was performed to avoid possible contaminations and the RNA was quantified through a UV spectrophotometer (ND-1000 UV-Vis, NanoDrop Technologies, USA). To assess the quality of the samples, reactions without the reverse transcriptase were made. The quality was evaluated. In this case the housekeeping gene *rpoD* was used, and only the samples with a C_T value higher than 30 would be used for further studies.

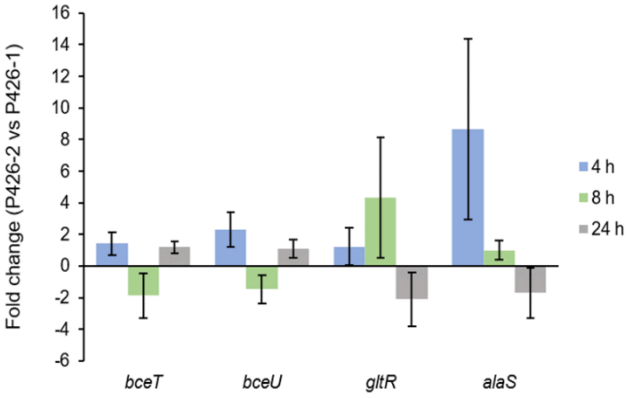

Figure 11: Expression levels of the target genes. Values are given in the form of C_T values) The columns represent mean $2^{-\Delta\Delta CT}$ values, the bars standard deviations.

The first mutation to be addressed is a 7-nucleotide insertion in the intergenic region between the two divergently transcribed genes, namely *bceT* and *bceU*. Considering a 2-fold cuttoff for significantly different expression, we can conclude that none of the genes seem to be affected. Previous analysis of cepacian biosynthesis by the two different isolates indicates that both are able to present the mucoid phenotype due to cepacian biosynthesis in yeast extract mannitol medium [27]. This result is in line with the expression data of *bceT* and *bceU* genes here

reported, although a quantitative analysis for exopolysaccharide should be done to confirm that they produced a similar amount.

Regarding the second region, a 10-nucleotide deletion that occurred between the divergently expressed genes *alaS* and *gltR*, could affect the expression of both genes at 8 hours of growth. Nevertheless, the standard error is very high, and no definite conclusion can be taken without repeating this experiment.

Conclusion and future perspectives

In conclusion there are 7 mutations distinguishing the two clinical isolates, four SNP mutations in coding regions, which were in a gene encoding a putative quorum-quenching lactonase (YtnP), an efflux pump (PbuE), a multidrug resistance protein (Stp) and an outer membrane protein (TtgC). Between the two isolates there are also a large deletion of hypothetical proteins and two small indel mutations in intergenic regions, being the genes that could be affected by these mutations the UTP-glucose-1- phosphate uridylyltransferase (BceT) and acetyltransferase (BceU), and a LysR-type transcriptional regulator (GltR) and an alanyl-tRNA synthetase (AlaS).

Previous phenotypic characterization of P0426-1 and P426-2 identified a few differences between them, namely a decreased swimming and swarming motility and increased resistance to ciprofloxacin by the P0426-2 isolate [27]. Other phenotypes such as the presence of O antigen in the lipopolysaccharide, antimicrobial resistance against several antibiotics, the mucoid phenotype, adhesin to CF lung epithelial cells and virulence in *Galleria mellonella* showed no significant differences. The increased resistance to ciprofloxacin by P0426-2 isolate could be caused by mutation in genes such as *pbuE*, *stp* or *ttgC*. But differences in motility and aggregate formation might be more likely caused by quorum sensing regulation. For that reason, the most evident target would be gene *ytnP* encoding a putative lactonase.

A complementation assay was performed to test whether expression of a different form of the lactonase in *B. multivorans* P0426-1 would affect aggregates formation. The expression of YtnP-85R in P0426-1 did not prevent aggregate formation, but the structure of the aggregates was more compact and with more ramifications. Furthermore, the comparison of the aggregates biomass between P0426-1/ pBBR1MCS and P0426-1-YtnP-85R showed a statistically significant reduction (53% to 22%) for the isolate expressing YtnP-85R. In addition, the complementation of isolate P0213-1 with YtnP-85R also showed macroscopic and microscopic changes. This result suggests that YtnP-85R expression might have affected both the structure of the aggregates and the relative amount. Although the expression of YtnP-85R in P0426-1 and P0213-1 did not abolish aggregation of cells, this preliminary data provides good indications that this novel lactonase might be relevant in the regulation of Burkholderia pathogenesis. Future studies will involve the construction of a YtnP deletion mutant; studies on expression of this gene during the growth phases; determination of the range of AHLs being degraded by this lactonase; and measure the intracellular levels of AHLs in the presence and absence of YtnP. As a final remark, is important to say that despite the observed mutations, their effect on aggregates formation might be an indirect one, for example through regulation of gene expression. In that case, perhaps determining the transcriptome of the two isolates would give us some clues on this virulence mechanism.

References

1. Polgreen, P. M., Brown, G. D., Hornick, D. B., Ahmad, F., London, B., Stoltz, D. A., & Comellas, A. P. (2018). CFTR Heterozygotes Are at Increased Risk of Respiratory Infections: A PopulationBased Study. Open Forum Infectious Diseases, 5(11).
2. Cant, N., Pollock, N., & Ford, R. C. (2014). CFTR structure and cystic fibrosis. The International Journal of Biochemistry & Cell Biology, 52, 15–25.
3. Naehrig, S., Chao, C.-M., & Naehrlich, L. (2017). Cystic Fibrosis [JD]. Dtsch Arztebl Int., 114(33- 34): 564–574.
4. Fanen, P., Wohlhuter-Haddad, A., & Hinzpeter, A. (2014). Genetics of cystic fibrosis: CFTR mutation classifications toward genotype-based CF therapies. The International Journal of Biochemistry & Cell Biology, 52, 94–102.
5. Sheppard, M. N., & Nicholson, A. G. (2002). The pathology of cystic fibrosis. Current Diagnostic Pathology, 8(1), 50–59.
6. Inglis, S. K., Corboz, M. R., & Ballard, S. T. (1998). Effect of anion secretion inhibitors on mucin content of airway submucosal gland ducts. American Journal of Physiology-Lung Cellular and Molecular Physiology, 274(5), L762–L766.
7. Engelhardt, J. F., Yankaskas, J. R., Ernst, S. A., Yang, Y., Marino, C. R., Boucher, R. C., Cohn, J. A., & Wilson, J. M. (1992). Submucosal glands are the predominant site of CFTR expression in the human bronchus. Nature Genetics, 2(3), 240–248Hollmann, B., Walsh, D. and Perkins, M., n.d. Biofilms And Their Role In Pathogenesis.
8. Yin, W., Wang, Y., Liu, L., & He, J. (2019). Biofilms: The Microbial "Protective Clothing" in Extreme Environments. International Journal of Molecular Sciences, 20(14), 3423.
9. Schleheck, D., Barraud, N., Klebensberger, J., Webb, J. S., McDougald, D., Rice, S. A., & Kjelleberg, S. (2009). *Pseudomonas aeruginosa* PAO1 Preferentially Grows as Aggregates in Liquid Batch Cultures and Disperses upon Starvation. PLoS ONE, 4(5), e5513.
10. Schwab, U., Abdullah, L. H., Perlmutt, O. S., Albert, D., Davis, C. W., Arnold, R. R., Yankaskas, J. R., Gilligan, P., Neubauer, H., Randell, S. H., & Boucher, R. C. (2014). Localization of *Burkholderia cepacia* Complex Bacteria in Cystic Fibrosis Lungs and Interactions with Pseudomonas aeruginosa in Hypoxic Mucus. Infection and Immunity, 82(11), 4729–4745.
11. Meade, H. M., Long, S.R., Ruvkun, G. B., Brown, S. E., Ausubel, F. M. 1982. Physical and genetic characterization of symbiotic and auxotrophic mutants of *Rhizobium meliloti* induced by transposon Tn5 mutagenesis. J Bacteriol 149:114–122.
12. J. S., Russel, D.W. 2001. Molecular cloning: a laboratory manual. New York.
13. Gomes, S. C. (2018). Genetic and environmental conditions influencing cellular aggregates formation in Burkholderia multivorans. Master Thesis from Instituto Superior Técnico.
14. Chan, K.-G., Wong, C.-S., Yin, W.-F., Sam, C.-K., & Koh, C.-L. (2010). Rapid degradation of N3-oxo-acylhomoserine lactones by a *Bacillus cereus* isolate from Malaysian rainforest soil. Antonie van Leeuwenhoek, 98(3), 299–305.
15. Kvist, M., Hancock, V., & Klemm, P. (2008). Inactivation of Efflux Pumps Abolishes Bacterial Biofilm Formation. Applied and Environmental Microbiology, 74(23), 7376–7382.
16. Baugh, S., Ekanayaka, A. S., Piddock, L. J. V., & Webber, M. A. (2012). Loss of or inhibition of all multidrug resistance efflux pumps of *Salmonella enterica* serovar Typhimurium results in impaired ability to form a biofilm. Journal of Antimicrobial Chemotherapy, 67(10), 2409–2417.
17. Sause, W. E., Balasubramanian, D., Irnov, I., Copin, R., Sullivan, M. J., Sommerfield, A., Chan, R., Dhabaria, A., Askenazi, M., Ueberheide, B., Shopsin, B., van Bakel, H., & Torres, V. J. (2019). The purine biosynthesis regulator PurR moonlights as a virulence regulator in Staphylococcus aureus. Proceedings of the National Academy of Sciences, 116(27), 13563–13572.
18. Goncheva, M. I., Flannagan, R. S., Sterling, B. E., Laakso, H. A., Friedrich, N. C., Kaiser, J. C., Watson, D. W., Wilson, C. H., Sheldon, J. R., McGavin, M. J., Kiser, P. K., & Heinrichs, D. E. (2019). Stress-induced inactivation of the Staphylococcus aureus purine biosynthesis repressor leads to hypervirulence. Nature Communications, 10(1).
19. Pasqua, M., Bonaccorsi di Patti, M. C., Fanelli, G., Utsumi, R., Eguchi, Y., Trirocco, R., Prosseda, G., Grossi, M., & Colonna, B. (2021). Host - Bacterial Pathogen Communication: The Wily Role of the Multidrug Efflux Pumps of the MFS Family. Frontiers in Molecular Biosciences, 8.
20. Ferreira, A. S. (2011). Insights into the role of extracellular polysaccharides in Burkholderia adaptation to different environments. In Frontiers in Cellular and Infection Microbiology (Vol. 1). Frontiers Media SA.
21. Ferreira, A. S., Leitão, J. H., Sousa, S. A., Cosme, A. M., Sá-Correia, I., & Moreira, L. M. (2007). Functional analysis of Burkholderia cepacia genes bceD and bceF , Encoding a phosphotyrosine phosphatase and a tyrosine autokinase, respectively: role in exopolysaccharide biosynthesis and biofilm formation. In Applied and Environmental Microbiology (Vol. 73, Issue 2, pp. 524–534). American Society for Microbiology.
22. Ferreira, A. S., Silva, I. N., Oliveira, V. H., Becker, J. D., Givskov, M., Ryan, R. P., Fernandes, F., & Moreira, L. M. (2013). Comparative transcriptomic analysis of the Burkholderia cepacia tyrosine kinase bcef mutant reveals a role in tolerance to stress, biofilm formation, and virulence. In Applied and Environmental Microbiology (Vol. 79, Issue 9, pp. 3009–3020). American Society for Microbiology.
23. Lee, J., & Zhang, L. (2014). The hierarchy quorum sensing network in Pseudomonas aeruginosa. Protein & Cell, 6(1), 26–41.
24. Rémy, B., Plener, L., Decloquement, P., Armstrong, N., Elias, M., Daudé, D., & Chabrière, É. (2020). Lactonase specificity is key to quorum quenching in Pseudomonas aeruginosa. In Frontiers in Microbiology (Vol. 11). Frontiers Media SA.
25. Sio, C. F., Otten, L. G., Cool, R. H., Diggle, S. P., Braun, P. G., Bos, R., Daykin, M., Cámara, M., Williams, P., & Quax, W. J. (2006). Quorum quenching by an n -acyl-homoserine lactone acylase from Pseudomonas aeruginosa PAO1. In Infection and Immunity (Vol. 74, Issue 3, pp. 1673–1682). American Society for Microbiology.
26. Malešević, M., Stanisavljević, N., Novović, K., Polović, N., Vasiljević, Z., Kojić, M., & Jovčić, B. (2020). Burkholderia cepacia YtnP and Y2-aiiA lactonases inhibit virulence of Pseudomonas aeruginosa via quorum quenching activity. Microbial Pathogenesis, 149, 104561.
27. Pessoa, Filipa Duarte. 2017. "Long-term evolution of Burkholderia multivorans bacteria during chronic respiratory infections of cystic fibrosis patients," Master Thesis, Instituto Superior Técnico.
28. Figurski, D. H., & Helinski, D. R. (1979). Replication of an origin-containing derivative of plasmid RK2 dependent on a plasmid function provided in trans. Proceedings of the National Academy of Sciences, 76(4), 1648–1652.
29. Kovach, M. E., Phillips, R. W., Elzer, P.H., Roop, R. M. II, Peterson, K. M. (1994). pBBR1MCS: a broad-host-range cloning vector. Biotechniques 16:800–802.

Supplementary data

Table S1: Bacterial strains and plasmids

Strains or plasmids	Description	Reference or source
Bacterial strains – *Burkholderia multivorans*		
P0426-1	Cystic fibrosis isolate, Canada	D.P. Speert University of British Columbia
P0426-2	Cystic fibrosis isolate, Canada	D.P. Speert University of British Columbia
P0213-1	Cystic fibrosis isolate, Canada	D.P. Speert University of British Columbia
P0148-1	Cystic fibrosis isolate, Canada	D.P. Speert University of British Columbia
Bacterial strains – *Escherichia coli*		
DH5-α	DH5α recA1 Δ(lacZYA-argF)U169 ϕ80dlacZΔM15	Gibco BRL
Plasmids		
pBBR1MCS	4,717-bp broad-host-range cloning vector, Cm^r	[28]
pRK2013	Tra+ Mob+ (RK2) Km::Tn7 ColE1 origin, helper plasmid, Km^r	[29]
pCR20-1	pBBR1MCS derivative containing a fragment with the *ytnP* gene from P0426-1	This work
pCR20-5	pBBR1MCS derivative containing a fragment with the *ytnP* gene from P0426-2	This work

Abbreviations: Cm^r, chloramphenicol resistance; Km^r , kanamycin resistance

Table S2: Primers

Primers	Foward	Reverse
Comp_YtnP	5’ GGGTACCAGATCGAACGTGAACTGCTGGA ’3	5’ CTCTAGAGGCGACCTTTCACCAATTGTCA ’3
PromTtgC	5’- GGGTACCTCGTGAAGCTGCTCGTGTCGA - 3’	5’ – CTCTAGAGGCAGTGCGGATTTCAGGA – 3’
Comp_TtgC	5’- GGATATCGTGTTCTACGTCGTGCTGC - 3’	5’ – CTCTAGAACTTCATGTGCGCAGCGGC – 3’
Purf_YtnP	5’-CGCTAGCAGCGCAACCATCCACAATGT-3’	5’– CCTCGAGGTAATCCCACGTCACGGGTA – 3’
RT-qPCR		
GalU	5’ ATGATCCTCGATCGCGCGCTTG’3	5’ GTCGTCGACAAGCCGCTGATCC ’3
OatA	5’ ACTGGATCGGCGTCGTGAAGGA ’3	5’ CACGAGCGGCGCGATCAGATAG ’3
GltR	5’ GCTCGCGATCTTCTCGGCTTCC ’3	5’ TGAGCACTTTCCCGAACGCACC ’3
AlaS	5’CGAGATGGAGTCCGATGCACGC’3	5’ GTAGACGGCCTTGCGCTCGATC ’3

Table S3: Mutations identified between *B. multivorans* P0426-1 and P0426-2.

Annotation	Location	Locus tag	Aminoacid	Effect in protein	Type of mutation	P426-1	P426-2	Nº of isolates with mutation
Putative quorum-quenching lactonase (YtnP)	CDS	FEP59_00467	S>R	nonsyn	SNP	T	G	20
Purine efflux pump (PbuE)	CDS	FEP59_00501	L>M	nonsyn	SNP	G	T	20
Multidrug resistance protein (Stp)	CDS	FEP59_00575	Q>P	nonsyn	SNP	A	C	1
Toluene efflux pump outer membrane protein (TtgC)	CDS	FEP59_01688	T>A	nonsyn	SNP	T	C	20
Between FEP59_02506 and FEP59_02507	IG	-	-	-	Indel	-	+7cgaacgc	10
Between FEP59_04039 and FEP59_04040	IG	-	-	-	Indel	-	-10cacgcaggct	20
Several hypothetical proteins	-	-	-	-	indel	-	del 44 kb	7

Coding region – CDS; Intergenic region – IG; Single-nucleotide substitution – SNP; Synonymous mutation – Syn; Non-synonymous – Nonsyn